11th Australasian Fluid Mechanics Conference
University of Tasmania, Hobart, Australia
14-18 December 1992

SOME EXPERIMENTAL STUDIES OF VORTEX RINGS GENERATED AT TUBE AND ORIFICE OPENINGS USING PARTICLE IMAGE VELOCIMETRY

T.T. LIM[1], R.F. LaFONTAINE[2], I.C. SHEPHERD[2] and A.E. PERRY[1]

[1]Dept Mechanical & Manufacturing Engineering, University of Melbourne, Parkville, VIC 3052, AUSTRALIA

[2]CSIRO Division of Building Construction & Engineering, PO Box 56, Highett, VIC 3190, AUSTRALIA

Abstract

Particle Image velocimetery has been used to measure the velocity fields of fully formed vortex rings generated at a tube and at an orifice openings. The aim is to study the topology of the vortex rings and to gain an insight into their entrainment processes. Another motivation is to determine the circulations of the vortex rings and to compare them with the predictions of the slug-flow model and the model of self-similar roll-up. This paper presents the preliminary results of our investigation.

Introduction

Until recently, most of the qantitative investigations on vortex rings have been carried out using either hot-wire or laser doppler anemometry. Unfortunately, these techniques suffer from the short coming that they provide only point by point measurements. Not only are they tedious and time consuming, the added difficulties of having to produce identical rings would inevitably lead to a washout of the measured data. In this study, Particle Image Velocimeter (PIV) is used. The attraction of this technique is that it enables simultaneous multipoint measurements to be carried out. Although the method has been used to study vortex rings before (for example, see Willert and Gharib(1991)), to the authors knowledge, very little attempt has been made towards understanding their topology. We believe that examining the toplogy may lead us to a better understanding of the entrainment processes in vortex rings. One of the objectives of this study is therefore to study the topology of the rings. Another objective is to determine their circulation and to compare them with the predictions of the slug-flow model and the model of self-similar roll-up. This paper presents the preliminary results of our investigation.

Experimental apparatus and procedure

The experimental layout is shown schematically in figure 1. The apparatus used for generating the vortex rings is essentially the same as that used by Lim (1989) but suitably modified for this study. It consists of two identical glass tanks (500 mm x 400 mm x 270 mm) with water as the working medium. One tank was fitted with a 31 mm diameter (D) orifice flush with one side of the wall and the other tank was equiped with a cone-edged tube of the same diameter which protudes about 5D inside the tank. Vortex rings were produced when the piston was advanced by a lead screw, driven by a high torque stepping motor. The motor was controlled by an IBM compatible PC to give a constant piston velocity over a predetermined time interval.

Velocity measurements were carried out using the PIV system developed by the CSIRO Division of Building, Construction and Engineering at Highett. Detailed description of the technique is given in Shepherd and LaFontaine (1992). Briefly, to use this technique the flow has to be seeded with particles which are assumed to follow the local velocity of the flow. By taking multiple exposures of the suspended particles with a known illumination function, it is possible to obtain images of the particle streaks which can later be Fourier transformed to obtain velocity vectors. In this experiment, the flow is seeded with fluorescent polymer spheres of approximately 80 μm diameter and with the specific gravity of ≅ 1.0. The seeding density is about 5 particles in a 32 x 32 pixel sampling window. To illuminate a plane of interest, a laser beam from a 5 watt argon ion laser is directed through an acousto-optic modulator (AOM) to a cylindrical lens whereby it is expanded into a sheet of light of about 1mm in thickness. The AOM, stepping motor and camera shutter operations were synchronised under the control of an Intel 80486 based personal computer. The profile of illumination was a single burst taking the form

$$I=\sin^2\left(\frac{\pi n t}{T}\right)\left(1-\frac{t}{T}\right)$$

where I is the light intensity, n is the number of cycles, t is the time ($t < T$) and T is the total window duration. The value of T is determined by the speed of the flow and in this experiment is between 50 and 300 msec. In theory, only 2 illumination cycles are needed for each burst,

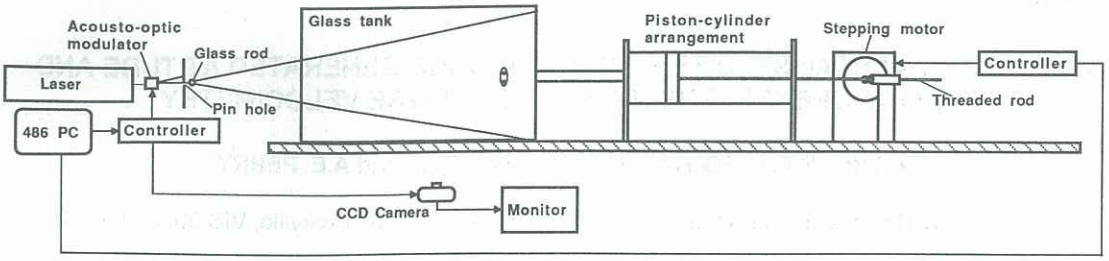

Figure 1 Schematic layout of apparatus

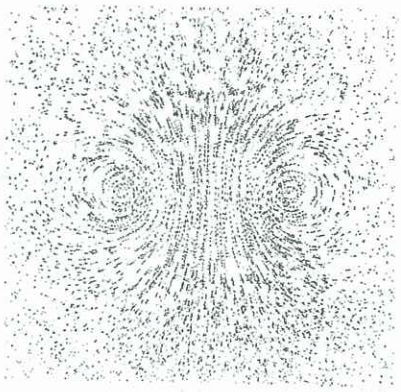

Figure 2. A typical particle streak pattern for a vortex ring generated at the tube. Here, the Reynolds number is 5800, L/D=1.32 and the illumination time is 100ms.

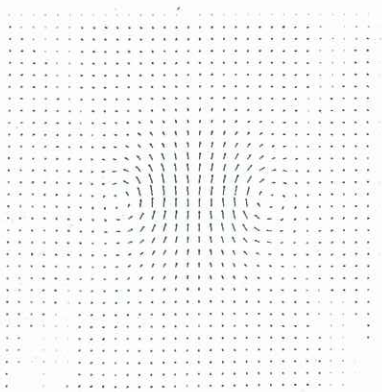

Figure 3. A complete velocity vector field of the ring as in figure 2. This is obtained by combining all the velocity vectors conducted for different illumination time.

however, in this study, 9 cycles was chosen because this improves the quality of the fringes after the Fourier transform. Moreover, the asymmetrical nature of the illumination function means that the sense of the velocity vectors can also be determined without any ambiguity.

To capture the image of the particle streaks, a Videk Megaplus charge-coupled device (CCD) camera was used and the image input to the PC via a Univision frame buffer/display. The digitized image has an area of 1280 pixels wide and 1024 pixels high which corresponds to the physical area of 12 cm by 9.6 cm.

In this study, the Reynolds number of the rings, UD/ν, based on the ejection velocity and the diameter of the nozzle, were 4600 and 5800 where ν is the kinematic viscosity. For each Reynolds number, the values of L/D chosen were 1.32 and 2.30 where L is the length of the "slug of fluid " ejected through the nozzle and is obtained from the distance travelled by the piston multiplied by the area ratio of the piston and the nozzle. All measurements were carried out at 5D from the exit plane of the nozzle.

Results and Discussions

Figure 2 shows a typical field of particle streaks obtained using a 100 millisecond exposure. The velocity vectors are retrieved by taking the Fourier tranform of the particle streaks using a 48 x 48 pixel with approximately 28% overlap between windows. When a large illumination time is used, only the first few streaks for each particle are used for analysis. This is to avoid the error due to streak curvature which may be introduced into the results when long exposure is used. A complete velocity field is obtained when all the velocity vectors for different parts of the flow are combined together. Figure 3 shows a typical velocity field retrieved on a 32 x 32 pattern.

(a) Circulation

To obtain the circulation for each ring, numerical intergration of the velocity is carried out around a closed circuit encompassing one vortex core. Figures 4 and 5 show the plots of the circulations of the rings versus L/D for the tube and the orifice opening respectively. These results have been non-dimensionalized with the circulation obtained using the slug-flow model. The solid curve represents the prediction using the self-similar roll-up model of Pullin(1979). For comparison, the experimental results of Maxworthy (1977) and Didden (1979) obtained using laser doppler anemometry have also been included. It is of interest to note that for the tube opening, our results closely followed those of Didden and show that both the slug model and the self-similar roll-up model of Pullin understimate the measured circulation of the ring. For the case of the orifice opening, our study also shows that the slug model underestimates the actual circulation of the ring, however, more data is needed in order to make a sensible comparison with the model of Pullin.

Figures 4 and 5 also show that, for both the tube and orifice openings, the circulations of the rings appear to be insensitive to the Reynolds number of the flow and seem to

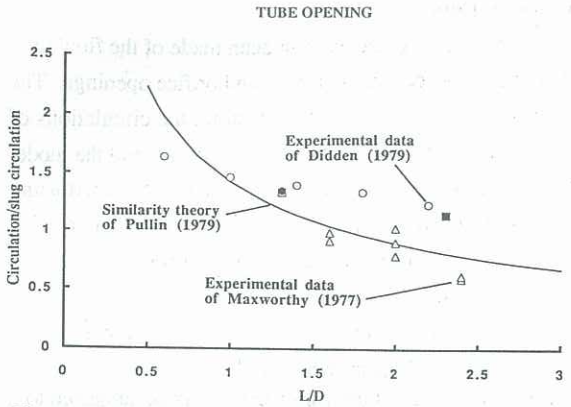

Figure 4. Circulation of a range of vortex rings generated at the tube for different values of L/D. Open squares and solid circles are results obtained by the present authors for Re=4600 and Re=5800 respectively. The data for the two Reynolds numbers almost coincide.

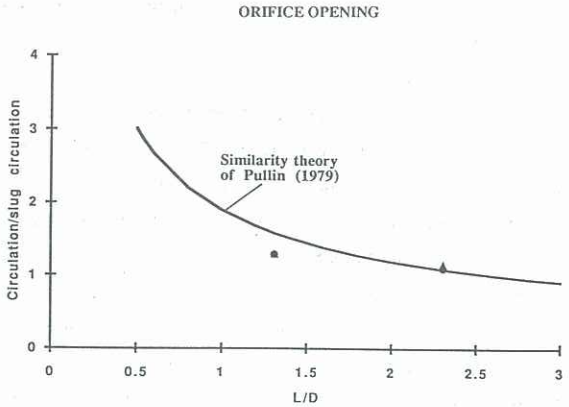

Figure 5. Circulation of a range of vortex rings generated at the orifice for different values of L/D. Solid circles and solid triangles are results obtained by the present authors for Re=4600 and Re=5800 respectively. The data for the two Reynolds numbers are very close together.

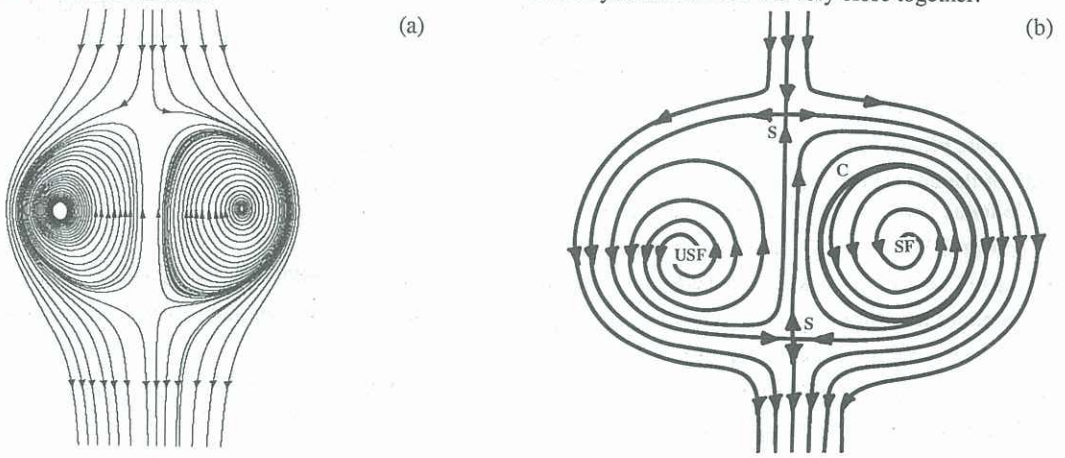

Figure 6. (a) Integrated streamline pattern of the vortex ring generated at the tube. Re=5800 , L/D= 1.32. (b) Authors' intepretation of (a). S - saddle, SF - stable focus, USF - unstable focus, C - limit cycle.

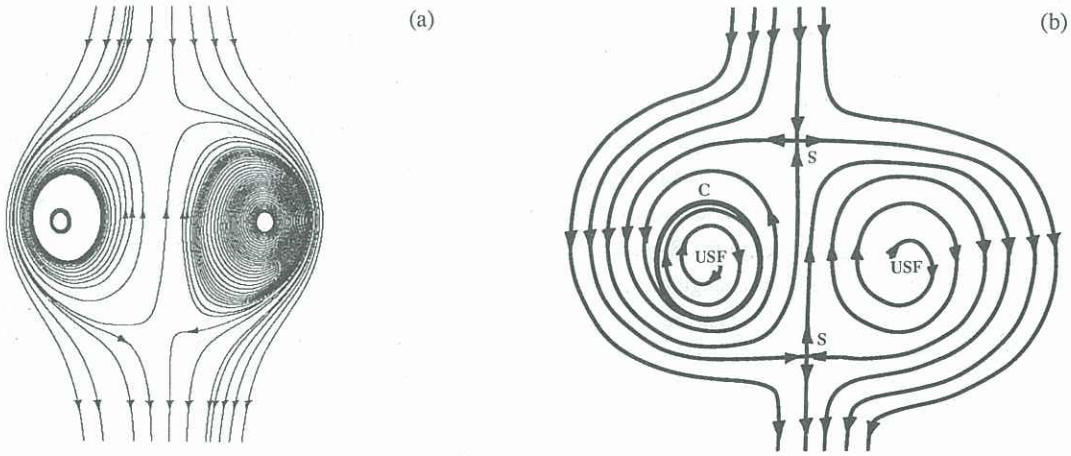

Figure 7. (a) Integrated streamline pattern of the vortex ring generated at the orifice. Re= 5800, L/D= 2.30. (b) Authors' intepretation of (a). S - saddle, USF - unstable focus, C - limit cycle.

depend only on L/D. This is consistent with the findings of Didden.

(2) Flow topology

The topology of the vortex ring is studied by locating the critical points in the velocity field. To accomplish this, the velocity vectors such as that shown in figure 3 is smoothed using a bi-axial 5-point smoothing technique. The smoothed data is then splined using a two-dimensional piecewise-cubic B-spline scheme which enables intergrated streamlines to be plotted using a modified predictor-corrector integration scheme (see Perry & Steiner (1987)). Figures 6(a) and 7(a) show the resultant streamline patterns obtained for the vortex rings generated at the tube for L/D=1.32 and 2.30 respectively. These patterns are seen by an observer moving with the convection velocity of the rings. Here, the convection velocity is determined by taking two successive dye images of the ring over a predetermined time. For clarity, the authors' interpretations of the streamline patterns are depicted in figures 6(b) and 7(b).

In figure 6(b), it can be seen that the streamlines in the vicinity of the left hand vortex core are spiralling out (i.e unstable focus) whereas, near the right hand core, a limit cycle appears. Within the limit cycle, the streamlines are spiralling in (i.e. stable focus) and outside the limit cycle, the streamlines are spiralling out. Interestingly, in figure 7(b), a limit cycle appears on the left instead and an unstable focus is now on right. Moreover, unlike the limit cycle in figure 6, the streamlines here are spiralling out inside the limit cycle and the streamlines are spiralling in outside the limit cycle. Although not shown here, vortex rings generated at the orifice opening appear to show a similar behaviour. The spiralling in of the streamlines indicates that the vortex core is being stretched and the ambient fluid is entrained into the ring. Conversely, the spiralling out of the streamlines indicates that the vortex core is being compressed and the fluid is ejected into the wake. Although the results shown in figures 6 and 7 are for different values of L/D, the observed behaviour of these rings leads us to speculate that vortex rings may be oscillating as they propogate through the fluid. Also, the vortex cores may be subjected to a changing rate of strain around the circumference of the rings, thus causing the fluid to be entrained or ejected from the ring. In making the above interpretation, we are fully aware of the pitfalls associated with interpreting a three-dimensional flow from a velocity field obtained from a two-dimensional slice. A possible way of verifying our interpretation is to follow the vortex ring using a movie camera so that the time variation of the streamline pattern can be determined.

Conclusions

Experimental studies have been made of the flow field of vortex rings generated at tube and orifice openings. The results show that for the tube opening, the circulations of the rings obtained using the slug-flow model and the model of self-similar roll-up underestimate those obtained using PIV and those obtained by Didden. For the orifice opening, the slug-flow model also shows lower values than the actual circulations.

Based on the information obtained so far, it would appear that the rings may be oscillating as they propogate through the fluid and the vortex cores may be subjected to a changing rate of strain field, thus causing the fluid to be either entrained or ejected from the ring. Further work is needed to verify this behaviour.

Acknowledgement:

The authors, T.T. Lim and A.E.Perry, acknowledge the support of the Australian research Council.

References:

Didden, N. 1979. On the formation of vortex rings:Rolling up and production of circulation. Z.Agnew. Math. Phys. **30**, 101-116.

Lim, T.T. 1989. An experimental study of a vortex ring interacting with an inclined wall. Exp. Fluids **7**, 453-463.

Maxworthy, T. 1977. Some Experimental studies of vortex rings. J. Fluid Mech. **81**, pp. 465-495.

Perry, A.E. and Steiner,T.R. 1987. Large-scale vortex structures in turbulent wakes behind bluff bodies. Part 1. Vortex formation processes. J. Fluid Mech. **174**, pp. 233-270.

Pullin, D.I. 1979. Vortex ring formation at tube and orifice openings. Phys. Fluids **22**, pp.401-403.

Shepherd, I.C. and LaFontaine, R.F. 1992. Mapping instantaneous velocity field using Particle Image Velocimetry. Eleventh Australasian Fluid Mechanics Conference, Hobart, Australia.

Willert, C.E. and Gharib, M. 1991. Digital particle image velocimetry. Experiments in Fluids **10,** pp.181-193.